Mice Lacking GPR88 Show Motor Deficit, Improved Spatial Learning and Low Anxiety Reversed by Delta Opioid Antagonist

Supplement 1

Supplemental Methods and Materials

Construction of Floxed GPR88 Mice

Gpr88 floxed mice (*Gpr88*$^{fl/fl}$) were generated at the Institut Clinique de la Souris using Cre-LoxP technology. We first generated mice with a floxed *Gpr88* gene (*Gpr88*$^{fl/fl}$) where exon 2 is flanked by a loxP site (upstream) and a Lox-FRT neomycin-resistance cassette (downstream) (Figure 1A). A 9.6 kb genomic clone containing exons 1 and 2 of the *Gpr88* gene was isolated from 129Sv genomic DNA and cloned into a targeting plasmid to generate the targeting vector. This clone was engineered to introduce a loxP site 230 bp upstream of exon 2 and 524 pb after the stop codon. The targeting vector was linearized for electroporation into 129Sv derived embryonic stem (ES) cells, which were selected with neomycin. Surviving cells were screened for homologous recombination by PCR. ES cells with the correct genotype were injected into C57BL/6J blastocysts, and resulting chimeric males were bred with C57BL/6J females to obtain germline transmission. F1 heterozygous *Gpr88*$^{fl/+}$ mice were bred with CMV-Flip mice in order to remove the neomycin cassette, and the obtained animals were then crossed with CMV-Cre mice expressing Cre recombinase under the cytomegalovirus promoter (1, 2). This led to germ-line deletion of Gpr88 exon 2 on a hybrid 50% C57BL/6J–50% 129Sv genetic background. We obtain *Gpr88*$^{fl/fl}$ x CMV-Cre$^{Tg/+}$ (deletion of *Gpr88* exon 2; *Gpr88*$^{-/-}$ mice), *Gpr88*$^{+/+}$ x CMV-Cre$^{0/+}$ (*Gpr88* wt allele; *Gpr88*$^{+/+}$), *Gpr88*$^{+/+}$ x CMV-Cre$^{Tg/+}$ and *Gpr88*$^{fl/+}$ x CMV-Cre$^{0/+}$ animals. *Gpr88*$^{-/-}$ and *Gpr88*$^{+/+}$ were used as experimental and control animals, respectively.

Behavioral Experiments

Experiments were performed on separate cohorts of naïve animals. Locomotor activity in open-field, novel object recognition and novelty suppressed feeding were performed in 4

equal square arenas (50 x 50 cm) separated by 35 cm-high opaque gray Plexiglas walls over a white Plexiglas platform (View Point, Lyon, France).

Locomotor Activity. Forward activity was monitored at 15 lx either in open fields placed over a white Plexiglas infrared-lit platform. Locomotor activity was recorded via an automated tracking system (videotrack; View Point, Lyon, France). Only movements for which speed was over 6 cm/s were taken into account for this measure.

Nest Building Behavior. Gpr88$^{+/+}$ and *Gpr88*$^{-/-}$ mice were single-housed overnight (16 h) in standard cages provided with a single housing-device (red plastic igloo; SDS Mazuri, Argenteuil, France) with three openings. A block of nesting material was placed in the opposite end of the cage. Each cage was scored by adding the number of openings covered (1, 2 or 3) with nesting material to the condition of this material: 1 for initiation of shredding and 2 for a totally shredded nesting block.

Motor Stereotypies. Mice were individually placed in clear standard cages (21×11×17 cm) filled with 3-cm deep fresh sawdust for 10 min (30 lx). Numbers of rearing, burying, allogrooming, circling episodes and total time spent burying were scored by direct observation.

Skill Motor Learning. The apparatus was a rotarod (Bioseb, Valbonne, France) accelerating from 4 to 40 rpm in 5 min (40 lx). The rod was covered with insulation tubing for better grip; final external perimeter was 5-cm. On day 1, mice were habituated to rotation on the rod at 4 rpm, until they were able to stay more than 180 s. From day 2 to day 5, mice were tested for three daily trials (60 s intertrial). Each trial started by placing the mouse on the rod and beginning rotation at constant 4 rpm-speed for 60 s. Then the accelerating program was launched, and trial ended for a particular mouse when falling off the rod. Time stayed on the rod was automatically recorded.

Y-maze Exploration. Spontaneous alternation was assessed in a Y-maze consisting of three Plexiglas arms (40 x 9 x 16 cm) covered with distinct patterns (15 lx). Each mouse was placed at the center of a maze and allowed to freely explore the maze for 5 min. The pattern of entries into each arm was quoted on video-recordings. Spontaneous alternations (SPA),

i.e., successive entries into each arm forming overlapping triplet sets, alternate arm returns (AAR) and same arm returns (SAR) were scored, and the percentage of SPA, AAR and SAR was calculated as following: total / (total arm entries -2) * 100.

Novel Object Recognition. The experiments were conducted in 4 equal square arenas (50 x 50 cm) separated by 35 cm-high opaque gray Plexiglas walls. Light intensity of the room was set at 15 lx to facilitate exploration and minimize anxiety levels. The floor was a white Plexiglas platform (View Point, Lyon, France), spread with sawdust. The room was equipped with an overhead video camera connected to a computerized interface, allowing visualization and recording of behavioral sessions on a computer screen in the adjacent room.

The experimental paradigm lasted for 2 days (3, 4). On day 1, the animals were placed in an arena for a 15 min-habituation session with two copies of an unfamiliar object (T-shaped plastic tubing, 1.5 x 3.5 cm). These objects were not used later for the recognition test. On day 2, the recognition test was performed, consisting of 3 trials of 10 minutes separated by 2 intertrial intervals of 5 minutes, during which the animals were returned to their home cage (see Figure 3B). On the first trial, or familiarization phase, the mice were presented with two copies of an unfamiliar object. On the second trial, or place phase, one of the two copies was displaced to a novel location in the arena. On the third trial, or object phase, the copy that had not been moved on the previous trial was replaced by a novel object. Stimuli objects used in all previous experiments were Lego bricks, plastic rings, dices or marbles (size 1.5-3 x 2-3 cm). The identity of the objects as well as the spatial location in which these objects were positioned was balanced between subjects. The number of visits and the time spent to explore each object were scored manually on video recordings. A visit was acknowledged when the nose of the mouse came in direct contact with an object. A percentage of discrimination was calculated for number of visits and time exploring the objects as following: exploration of displaced or novel object / total exploration * 100. The percentage of discrimination during familiarization phase was arbitrarily calculated for the object located in the right upper corner of the arena. Animals that failed to explore the objects more than 2 sec during the familiarization phase were excluded from further analysis, as well as mice that

failed to explore one of the objects during the place and object phases (one female *Gpr88*$^{-/-}$ mouse was excluded).

Cross Maze. Experiments were run in a cross-shaped maze, adapted from (5). Elevated 40 cm above the floor, the maze consisted of four arms (35 cm x 8 cm) with black Plexiglas floors enclosed in transparent Plexiglas walls (15 cm), except for the terminal half of west and east arms. Removable sliding doors made of black opaque Plexiglas delimited two starting boxes (10 x 8 cm) at the end of south and north arms. Four more identical sliding doors separated each arm from the central platform (8 x 8 cm). A food well (2 cm diameter) was inserted into the floor at 1 cm from the distal end of east and west arms. The maze was located in a testing room that contained several extra-maze visual cues, and maintained in a constant orientation during the experiment. Light intensity in the room was set at 15 lx. The floor and walls were cleaned regularly to limit intra-maze olfactory cues.

Place learning was evaluated using a dual-solution cross-maze task (3, 5-7). Mice were reduced to 85% of their *ad lib* feeding weights over 7 days before maze training and maintained at this weight throughout the experiment. The animals received sucrose reward tablets (5-10 per mouse; Formula 5TUT-formerly PJFSC-20 mg, TestDiet, Richmond, USA) in their home cage for three consecutive days before maze habituation. Habituation lasted three days, during which access to the north arm of the cross maze was blocked with a sliding door. The mice were placed in the south start box and allowed to explore the maze for 5 min. On day 1, sucrose tablets were available throughout the apparatus. On day 2, a trail of five tablets leading to the food cup was placed along the length of west and east arms. On day 3, tablets were present only in the food well at the end of baited arms.

Training (4 trials per day) started immediately after habituation. The north arm was closed and mice were released from the south arm, after a 15 s-confinement in the start box (see Figure 3). For half of the animals, single food-pellet bait was located in the east arm, while the other half of the animals received food in the west arm. After entering an arm, the door was closed and mice were confined for at least 20 s or until food was consumed. If a mouse failed to eat the food within 5 min, the trial was terminated. A correction procedure was used

during the first two training sessions only: mice making an incorrect response were allowed to trace back to the baited maze arm and consume the food pellet. Two parameters were recorded: choice accuracy was expressed as the percentage of entries in the baited arm during each session, and choice latency was recorded as the latency to enter an arm of the maze (baited or not).

Reversal was performed on session 15 and lasted for 7 sessions. Animals for which food was previously available in the east arm had to find the food bait in the west arm, and conversely. After entering an arm, the door was closed and mice were confined for at least 20 s or until food was consumed. If a mouse failed to eat the food within 5 min, the trial was terminated.

Probe trials were performed in the course of training to assess the strategy (place or response) used by the animals. Probe trials took place on sessions 8 and 17. Mice were released from the north arm and had access to the previously baited arm (place learning) or to the opposed arm (response learning). Food was available in both arms (see Figure 3C). Two parameters were recorded: choice accuracy was expressed as the percentage of entries in the baited arm during each session, and choice latency was recorded as the latency to enter an arm of the maze (baited or not).

Elevated Plus Maze. The EPM (Viewpoint®, Lyon, France) was a plus-shaped maze elevated 52 cm from base, with black Plexiglas floor, consisting of two open and two closed arms (37 x 6 cm each) connected by a central platform (6 x 6 cm). The walls of the closed arms were made of 18 cm-high clear acrylic. Light intensity in open arms was set at 15 lx. The apparatus was placed over an infrared-lit platform. The movement and location of the mice were analyzed by an automated tracking system equipped with an infrared-sensitive camera (videotrack; View Point, Lyon, France). All sessions were videotaped for further analyses.

Gpr88$^{+/+}$ and *Gpr88*$^{-/-}$ mice were exposed to the EPM for 5 min at 15 lx. Anxiety-like behavior was assessed by spatiotemporal and ethological measures (8). Automatically assessed spatiotemporal parameters included the distance traveled, time spent and number

of entries in closed and open arms, and related distance, time and activity ratios (distance or time spent or number of entries in open arms/total distance or time spent or number of entries in arms). The time spent in the distal part of the open arms was measured to evaluate risk assessment behavior. Ethological measures were scored manually (by an experimenter blind to genotype and treatment) on video recordings and included the frequency of stretched attend postures (SAP; exploratory posture in which the body is stretched forward but the animal's hind paws remain in position, followed by retraction to original position), flat back approaches (FBA; number of slow forward explorations with the body stretched) and head dips (HD; an exploratory behavior in which the animal scans over the sides of the maze towards the floor).

Marble Burying. Mice were introduced individually in standard cages covered with a filtering lid and containing 20 glass marbles (diameter: 1.5 cm) evenly spaced on 4-cm deep fresh sawdust (40 lux). After 15 min, the number of marbles buried more than half in sawdust was quoted (9).

Novelty-Suppressed Feeding. Novelty-suppressed feeding (NSF) was measured in 24-h food-deprived mice, isolated in a standard housing cage for 30 min before individual testing. Three pellets of ordinary lab chow were placed on a white tissue in the center of each arena, lit at 60 lx. Each mouse was placed in a corner of an arena and allowed to explore for a maximum of 15 min. Latency to feed was measured as the time necessary to bite a food pellet. Immediately after an eating event, the mouse was transferred back to home cage (free from cage-mates) and allowed to feed on lab chow for 5 min. Food consumption in the home cage was measured.

Drugs

For [^{35}S]-GTPgS binding, the GPR88 agonist Compound 19 (10) and glutamate were kindly synthetized by Prestwick Chemicals (Illkirch, France). (-)-Quinpirole hydrochloride (D2/3 agonist) and SNC-80 (delta opioid receptor agonist) were obtained from Tocris (Bristol, UK) and dissolved in saline (NaCl 0.9%) and dimethyl sulfoxide (DMSO) respectively.

Carbamylcholine chloride (carbachol, non selective cholinergic agonist) and [D-Ala2, N-MePhe4, Gly-ol]-enkephalin (DAMGO, mu opioid receptor agonist) were obtained from Sigma (St Louis, USA) and dissolved in water. For *in vivo* pharmacology, naltrindole hydrochloride (delta opioid receptor antagonist) was obtained from Tocris (Bristol, UK), dissolved in sterile saline solution (NaCl 0.9%) and injected daily subcutaneously in a volume of 10 ml/kg at 0.3 mg/kg (3, 11). Control animals received saline. Injections started 7 days before testing and continued until the end of the procedure. When undergoing behavioral testing, mice were injected 30 min before testing.

[^{35}S]-GTPgS Binding

To assess [^{35}S]-GTPgS binding in the whole striatal region, brains were quickly removed after cervical dislocation and the whole striatal region was dissected out, frozen in liquid nitrogen and stored at -80°C until use. Samples were rapidly frozen in liquid nitrogen and stored at -80°C until use. All assays were performed on membrane preparations. Four membrane preparations were used per genotype, each membrane preparation gathering tissue from three animals (1 male/2 females or 2 males/1 female, counterbalanced, see Table S2).

Membranes were prepared by homogenizing brain samples in ice-cold 0.25 M sucrose solution 10 vol (ml/g wet weight of tissue). The obtained suspensions were then centrifuged at 2500 *g* for 10 min. Supernatants were collected and diluted ten times in buffer containing 50 mM TrisHCl (pH 7.4), 3 mM $MgCl_2$, 100 mM NaCl, 0.2 mM EGTA, and then centrifuged at 23,000 *g* for 30 min. The pellets were homogenized in 800 µL ice-cold sucrose solution (0.32 M), aliquoted and kept at - 80°C until further use.

For [^{35}S]-GTPγS binding assays, 2 µg of protein were used per well. Samples were incubated with and without ligands, for 1 hour at 25°C in assay buffer containing 30 mM GDP and 0.1 nM [^{35}S]-GTPγS. Bound radioactivity was quantified using a liquid scintillation counter and Bmax and Kd values were calculated. Non-specific binding was defined as

binding in the presence of 10 µM GTPγS; basal binding refers to binding in the absence of the agonist. Data are expressed as a mean percentage of activation above this basal binding.

Real-Time Quantitative PCR Analysis

qRT-PCR was performed on brain samples as described previously (3, 9, 12). Mice were sacrificed by cervical dislocation; brains were rapidly removed and placed into a brain matrix (ASI Instruments, Warren, MI, USA). Caudate putamen (CPu), nucleus accumbens (NAc) and central amygdala (CeA) were punched as previously described (9). Prefrontal cortex (PFC) and CA1 of the dorsal hippocampus (CA1) were dissected out from two consecutive 1 mm-thick slices (Figure S1). Tissues were immediately frozen on dry ice and kept at -80°C until use. For each structure of interest and each genotype, tissue from one male and one female mouse was pooled in the same sample (*n* = 5 samples/genotype). RNA was extracted and purified using the MIRNeasy mini-kit (Qiagen, Courtaboeuf, France). cDNA was synthetized using the first-strand Superscript II kit (Invitrogen®, Life Technologies, Saint Thomas, France). qRT-PCR was performed in quadruplets on a LightCycler 480 Real-Time PCR (Roche, Manheim, Germany) using iQ-SYBR Green supermix (Bio-Rad, Marnes-la-Coquette, France) kit with 0.25 µl cDNA in a 12.5 µl final volume. Gene-specific primers were designed using Primer3 software to obtain a 100- to 150-bp product (see Table S1). Relative expression ratios were normalized to the level of actin and the $2^{-\Delta\Delta Ct}$ method was applied to evaluate differential expression level.

Neurochemical Assay for Biogenic Amine Dosage

Brains were placed into a cooled brain matrix and sliced. Bilateral punches of the CPu, NAc, CeA, ventral midbrain and unilateral punches of the dorsal raphe were removed from two consecutive 1 mm-thick brain slices (Figure S1). PFC and dorsal and ventral hippocampi were dissected out from two consecutive slices. Tissues were immediately frozen on dry ice and kept at -80°C until use. High performance liquid chromatography was used to measure

levels of biogenic amines described previously (9, 13). Values were expressed using the acquisition software Azur v4.5 (Datalys, St Martin d'Hères, France). Results were given as pg/µg of total protein (Lowry method).

DiI Staining and Quantification of Dendritic Spines

Male mice were anaesthetized deeply and then transcardially perfused with 50 ml of saline solution (0.9% NaCl), followed by 50 ml of an ice-cooled fixative solution containing 4% paraformaldehyde in 0.1 M phosphate buffer (PB), pH 7.5. The brains were removed, and postfixed in 4% paraformaldehyde for 24 h at 5°C, and rinsed in PB solutions. Brains were cut with a vibratome to obtain free-floating coronal brain sections of 70 µm that were collected in PBS 50 mM pH 7.4.

Lipophilic carbocyanine DiI crystals (1,1 -dioctadecyl-3,3,3',3'-tetramethylindocarbocyanine perchlorate; catalogue # D-282; Molecular Probes, Invitrogen, USA) were directly applied to the desired labeling brain regions under a dissecting microscope. Fine carbocyanine DiI crystals coated on the outer surface of a glass micropipette tip were delivered to the brain sections disposed on pieces of 70 µm nylon mesh filter, by lightly hitting the micropipette. Brain sections were maintained in PBS 50 mM pH 7.4 at room temperature for 24 h in the dark to allow fluorescent dye crystals to diffuse fully along the membranes of neuronal profiles. The DiI-labeled sections were post-fixed with PFA 4%; PBS 50 mM pH 7.4 for 30 min at room temperature, rinsed three times 10 min each and finally mounted on Superfrost slides using glycerol-based medium Mowiol (Calbiochem, La Jolla, USA).

Carbocyanine DiI-labeled neurons and dendritic spines were imaged using a Leica SP5 confocal laser scanning microscope. To visualize fluorescence emitted by DiI, a Helium/Neon 561 nm laser line was used. Each DiI-positive neuron and dendritic profiles that were well separated from neighboring neural processes were randomly sampled and imaged to be quantified. Special care was taken to ensure that each imaged distal dendritic segment belonged to a different neuron. All images were taken using the Plan-Apochromat

63 x oil-immersion objective with optical zoom 4 x (NA = 1.4). We used a frame size of 1024 x 1024 pixels. Serial stack images were scanned with step size of 0.13 µm along the z-axis (maximum 130 planes, depending on the depth of the distal dendritic profile), and then projected to reconstruct a three dimensional (3D) image.

For quantitative analysis, all 3D stacks were treated to remove noise from images using the quantification module of Volocity software package (Version 4.1, Perkin Elmer, USA) and then exported as a 3D stack Tiff file to the Neurolucida software (MBF Biosciences). Dendritic spine density was evaluated using the plug-in AutoSpine of Neurolucida software package (Version 7.51). Measurements were made to a maximum of 75 µm from the dendrite tip, and the minimum length of dendrite quantified was 50 µm. Both a series of stack images and a 3D projection image were used in a complimentary manner to increase the sensitivity of spine detection. Identified dendritic spines were counted in the 3D projection image interface. Whenever dendritic spines were too crowded to separate them from each other, we turned to serial stack images to identify individual spines with a greater certainty. All dendritic protrusions with a clearly recognizable stalk were counted as spines. For each animal at least ten neurons were analyzed. Spine number was divided by the length of dendritic segment to generate dendritic spine density expressed as number / µm. The average of spine density/10 µm for all dendritic segments captured per animal was used to yield the experimental value/spine density for that animal.

Statistical Analyses: qRT-PCR Data

qPCR data were transformed prior to statistical analysis to obtain a symmetrical distribution centered on 0, using the following formula: if $x<1$, $y=1-1/x$; if $x>1$, $y=x-1$ (x: qPCR data; y: transformed data) (12). A one-sample *t*-test was performed to assess statistical significance. Calculated *p* values indicated probability for a regulation to differ from 0. Unsupervised clustering analysis was performed on the median of transformed qPCR data using complete linkage with correlation distance (Pearson correlation) for genes and brain regions (Cluster 3.0 and Treeview software).

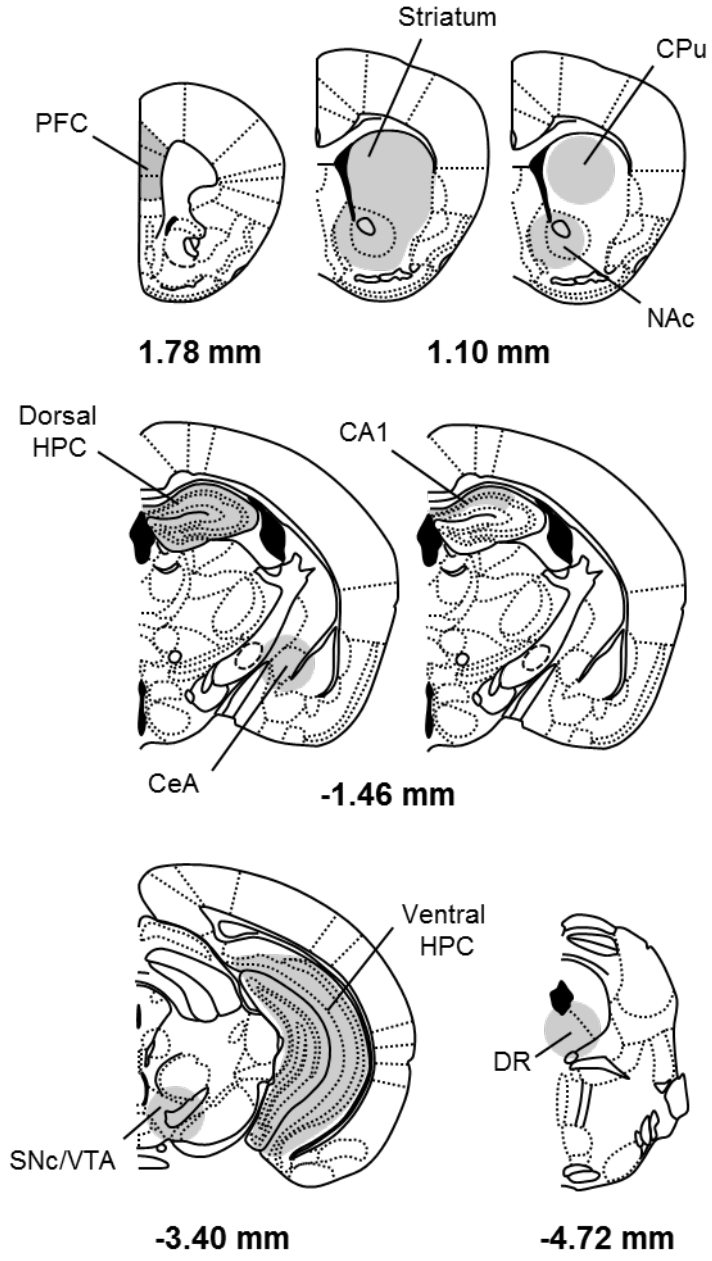

Figure S1. Schematic representations depict brain regions dissected for gene expression study, monoamine dosage and [^{35}S]-GTPγS binding. For qRT-PCR analysis, CPu, NAc and CeA were punched on 1-mm thick brain slices, whereas PFC and (dorsal) CA1 were dissected out from two consecutive slices. For monoamine dosage, CPu, NAc, CeA, SNc/VTA and DR were punched, PFC, dorsal and ventral HPC were dissected. Finally, for [^{35}S]-GTPγS binding assay, whole striatum and dorsal HPC were dissected whereas CPu, NAc and CeA were punched. CPu, caudate putamen; CeA, central amygdala; DR, dorsal raphe; HPC, hippocampus; NAc, nucleus accumbens; PFC, prefrontal cortex; SNc, substantia nigra, pars compacta; VTA, ventral tegmental area.

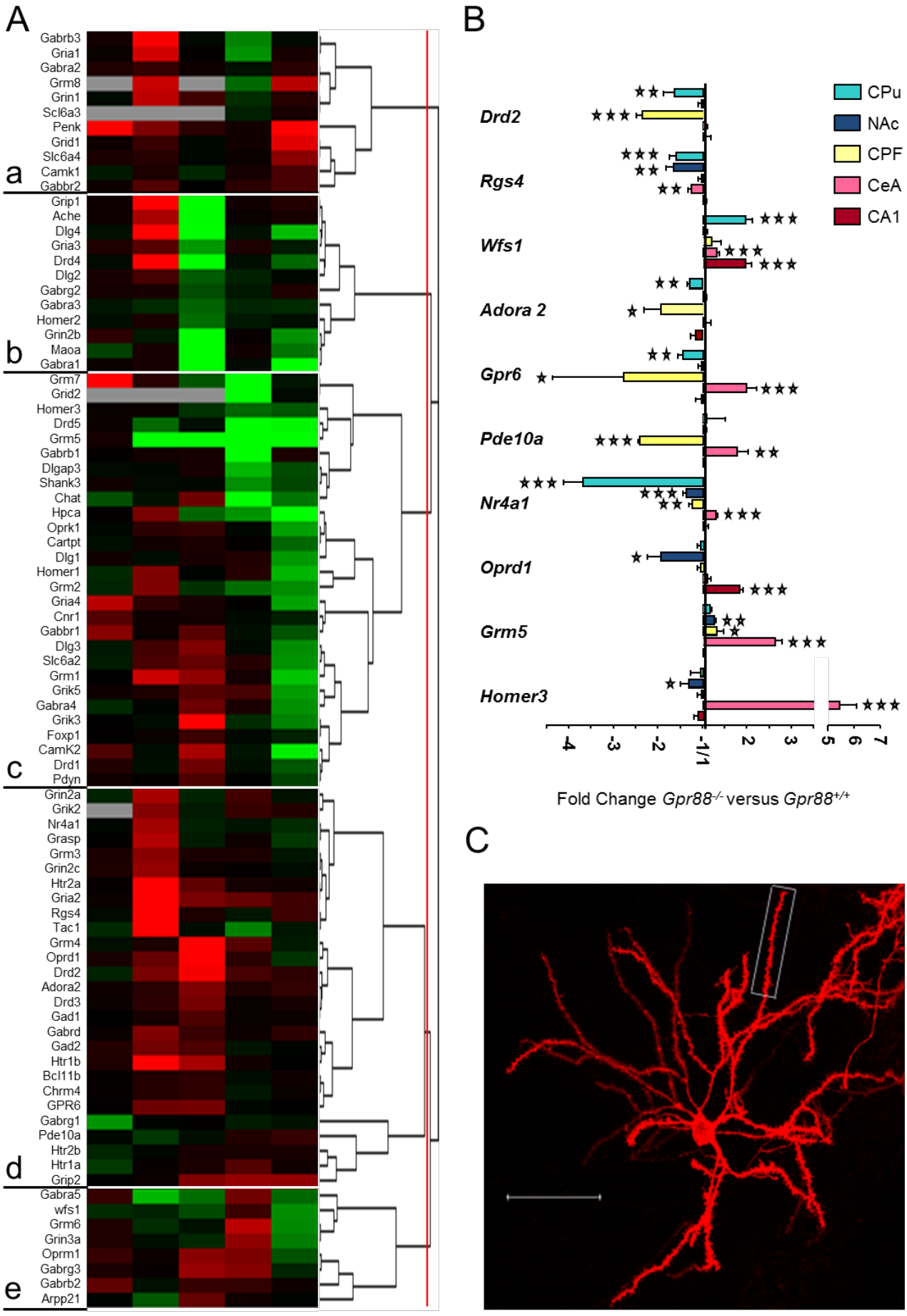
A
Gabrb3
Gria1
Gabra2
Grm8
Grin1
Scl6a3
Penk
Grid1
Slc6a4
Camk1
Gabbr2
a
Grip1
Ache
Dlg4
Gria3
Drd4
Dlg2
Gabrg2
Gabra3
Homer2
Grin2b
Maoa
Gabra1
b
Grm7
Grid2
Homer3
Drd5
Grm5
Gabrb1
Dlgap3
Shank3
Chat
Hpca
Oprk1
Cartpt
Dlg1
Homer1
Grm2
Gria4
Cnr1
Gabbr1
Dlg3
Slc6a2
Grm1
Grik5
Gabra4
Grik3
Foxp1
CamK2
Drd1
Pdyn
c
Grin2a
Grik2
Nr4a1
Grasp
Grm3
Grin2c
Htr2a
Gria2
Rgs4
Tac1
Grm4
Oprd1
Drd2
Adora2
Drd3
Gad1
Gabrd
Gad2
Htr1b
Bcl11b
Chrm4
GPR6
Gabrg1
Pde10a
Htr2b
Htr1a
Grip2
d
Gabra5
wfs1
Grm6
Grin3a
Oprm1
Gabrg3
Gabrb2
Arpp21
e
B
CPu
NAc
CPF
CeA
CA1
Drd2
Rgs4
Wfs1
Adora 2
Gpr6
Pde10a
Nr4a1
Oprd1
Grm5
Homer3
-4
-3
-2
-1/1
2
3
5
6
7
Fold Change Gpr88-/- versus Gpr88+/+
C

Figure S2. Clustering analysis identifies 5 main groups of genes sharing similar expression profiles in *Gpr88* null mice versus controls. (**A**) Transcript levels of 89 genes coding for key actors of GABA, glutamate and monoamine signaling pathways or striatal gene markers were assessed in the PFC, CPu, NAc, CeA and CA1 of mutant animals versus controls. Clustering analysis organized gene expression data in 5 main clusters (a-e). (**B**) Examples of individual gene expression profiles show region-specific regulation of transcription in *Gpr88*$^{-/-}$ mice. Gene names are displayed in Table S3. (**C**) Low magnification of a DiI fluorescent MSN in the striatum. The rectangle in the upper part delimitates a typical terminal dendritic segment used for analysis of spine density. Scale bar: 100 µm. CA1, CA1 of the dorsal hippocampus; CeA, central nucleus of the amygdala; CPF, prefrontal cortex; CPu, caudate putamen; NAc, nucleus accumbens.

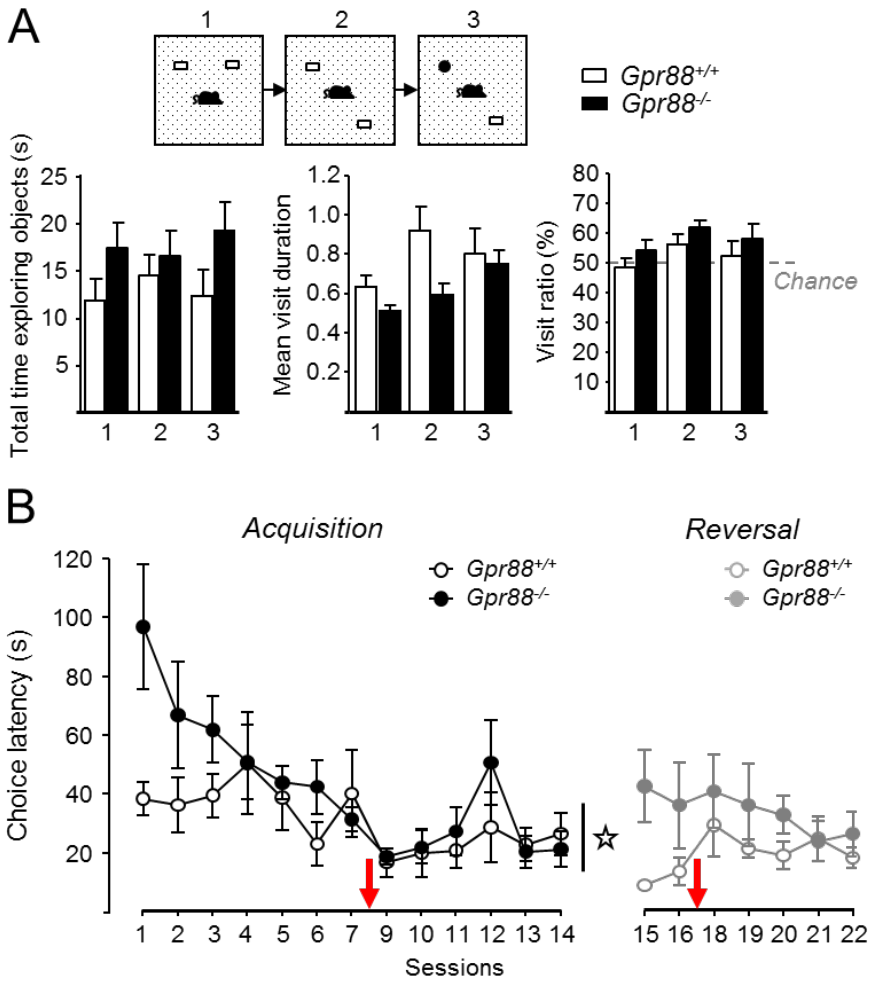

Figure S3. *Gpr88*$^{-/-}$ animals spend similar time exploring the objects in the novel object recognition test, but take longer to choose an arm in a dual-solution cross-maze task. (**A**) In the novel object recognition test, mutant and control mice display similar time exploring the objects, mean duration of visits and visit ratio, with visit duration increasing progressively across the 3 phases of the test; (**B**) *Gpr88*$^{-/-}$ mice display longer choice latencies, progressively shortening along sessions, during the acquisition of a dual-solution cross-maze task. Data are presented as mean ± SEM. Open star: genotype x session effect, $p < 0.05$.

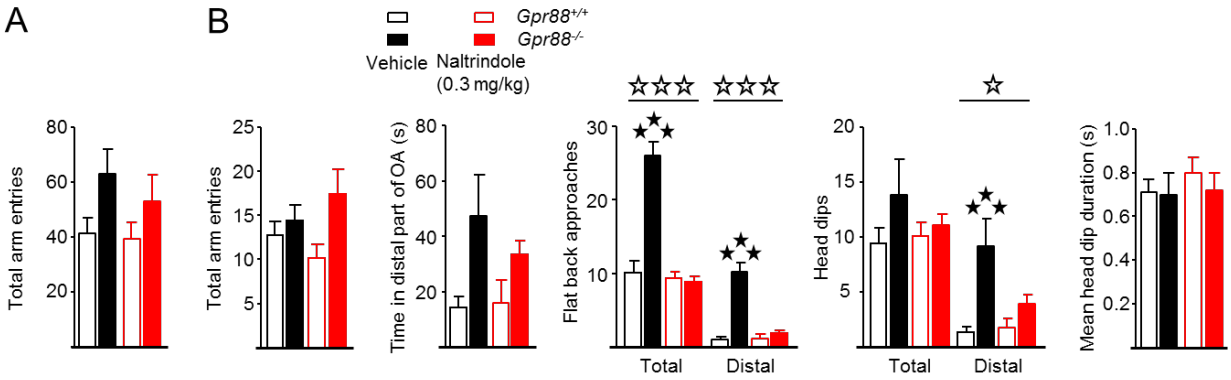

Figure S4. Chronic naltrindole treatment normalizes their behavioral profile in the Y-maze and EPM tests. (**A**) Chronic NTI administration failed to reduce augmented number of arm entries of *Gpr88*$^{-/-}$ mice in the Y-maze; (**B**) in the EPM test, NTI had no detectable effect on augmented number of arm entries (trend) and time spent in the distal part of OA in *Gpr88* null mice, whereas this treatment normalized their number of flat back approaches (total and distal) and distal head-dips; no difference was seen on the mean duration of head-dips.

Legends to Supplemental Tables (see Supplement 2, Excel file)

Table S1. List of primers used for qRT-PCR.

Table S2. Statistical analysis: [^{35}S]-GTPgS binding in *Gpr88*$^{-/-}$ and *Gpr88*$^{+/+}$ mice.

Table S3. Transcription of genes coding for a set of 89 genes, including main actors of GABA, glutamate or monoamine signaling and neuronal markers, was evaluated in the prefrontal cortex (PFC), caudate putamen (CPu), nucleus accumbens (NAc), central amygdala (CeA) and CA1 of the hippocampus (CA1) of *Gpr88*$^{-/-}$ mice versus controls. Data are presented as fold-change in *Gpr88*$^{-/-}$ versus *Gpr88*$^{+/+}$ mice (median ± SEM). Student's *t*-tests were performed on transformed data (see Methods and Materials) to determine whether fold changes differed from 0 (no regulation: corresponds to ± 1 in table). Significant regulations with a fold change over ± 1.25 are highlighted in bold (considered biologically significant). n.d., not detected.

Table S4. Bioamine concentrations in the prefrontal cortex, caudate putamen, nucleus accumbens, dorsal and ventral hippocampus, central nucleus of the amygdala, dorsal raphe and midbrain (SNc/VTA) of *Gpr88*$^{+/+}$ and *Gpr88*$^{-/-}$ animals. Serotonin (5HT), dopamine (DA), norepinephrine (NE), 3,4-dihydroxyphenylalanine acid (DOPAC) and 5-hydroxyindoleacetic acid (5HIAA) levels (pmol/µg protein) were determined in *Gpr88*$^{-/-}$ animals and their wild-type controls. Data are presented as mean ± SEM. n.d., not detected; SNc, substantia nigra, pars compacta; VTA, ventral tegmental area.

Table S5. Statistical analysis: behavioral phenotyping of *Gpr88*$^{-/-}$ versus *Gpr88*$^{+/+}$ mice. Behavioral phenotyping of *Gpr88* null mice as compared to wild-type counterparts was performed in independent naive cohorts of male and female animals, except for the grip test and string test, performed successively (in this order) in the same cohort. Trial effect was tested in the rotarod test; phase refers to trials 1 to 3 (familiarization, place and object phases) in object recognition. F, female; Geno, genotype; M, male.

Table S6. Statistical analysis: behavioral effects of chronic naltrindole (0.3 mg/kg) or saline treatment in *Gpr88*$^{-/-}$ and *Gpr88*$^{+/+}$ animals. Naltrindole (0.3 mg/kg, s.c.) or vehicle (saline) were administered daily for 7 days before the beginning of behavioral testing, and continued during the experiments. On testing days, injections were performed 30 min before behavioral assay. A first cohort of mutant and control animals underwent subsequently plus-maze testing (day 8) and novelty-suppressed feeding test (day 16). A second cohort was trained on the accelerating rotarod, starting day 8 after the beginning of treatment, and then tested for Y-maze exploration (day 24).

Supplemental References

1. Gaveriaux-Ruff C, Nozaki C, Nadal X, Hever XC, Weibel R, Matifas A, *et al.* (2011): Genetic ablation of delta opioid receptors in nociceptive sensory neurons increases chronic pain and abolishes opioid analgesia. *Pain*. 152:1238-1248.

2. Metzger D, Chambon P (2001): Site- and time-specific gene targeting in the mouse. *Methods*. 24:71-80.

3. Le Merrer J, Rezai X, Scherrer G, Becker JA, Kieffer BL (2013): Impaired hippocampus-dependent and facilitated striatum-dependent behaviors in mice lacking the delta opioid receptor. *Neuropsychopharmacology*. 38:1050-9.

4. Carey AN, Lyons AM, Shay CF, Dunton O, McLaughlin JP (2009): Endogenous kappa opioid activation mediates stress-induced deficits in learning and memory. *The Journal of Neuroscience*. 29:4293-4300.

5. Passino E, Middei S, Restivo L, Bertaina-Anglade V, Ammassari-Teule M (2002): Genetic approach to variability of memory systems: analysis of place vs. response learning and fos-related expression in hippocampal and striatal areas of C57BL/6 and DBA/2 mice. *Hippocampus*. 12:63-75.

6. Deipolyi AR, Fang S, Palop JJ, Yu GQ, Wang X, Mucke L (2008): Altered navigational strategy use and visuospatial deficits in hAPP transgenic mice. *Neurobiol Aging*. 29:253-266.

7. Packard MG (1999): Glutamate infused posttraining into the hippocampus or caudate-putamen differentially strengthens place and response learning. *Proc Natl Acad Sci U S A*. 96:12881-12886.

8. Sorregotti T, Mendes-Gomes J, Rico JL, Rodgers RJ, Nunes-de-Souza RL (2013): Ethopharmacological analysis of the open elevated plus-maze in mice. *Behav Brain Res*. 246:76-85.

9. Becker JA, Clesse D, Spiegelhalter C, Schwab Y, Le Merrer J, Kieffer BL (2014): Autistic-like syndrome in mu opioid receptor null mice is relieved by facilitated mGluR4 activity. *Neuropsychopharmacology*. 39:2049-60.

10. Dzierba CD, Bi Y, Dasgupta B, Hartz RA, Ahuja V, Cianchetta G, *et al*. (2015): Design, synthesis, and evaluation of phenylglycinols and phenyl amines as agonists of GPR88. *Bioorg Med Chem Lett*. 25:1448-1452.

11. Shippenberg TS, Chefer VI, Thompson AC (2009): Delta-opioid receptor antagonists prevent sensitization to the conditioned rewarding effects of morphine. *Biol Psychiatry*. 65:169-174.

12. Le Merrer J, Befort K, Gardon O, Filliol D, Darcq E, Dembele D, *et al.* (2012): Protracted abstinence from distinct drugs of abuse shows regulation of a common gene network. *Addiction Biology*. 17:1-12.

13. Goeldner C, Lutz PE, Darcq E, Halter T, Clesse D, Ouagazzal AM, *et al.* (2011): Impaired emotional-like behavior and serotonergic function during protracted abstinence from chronic morphine. *Biol Psychiatry*. 69:236-244.